ISSN: 2538-5887; Pathobiology Research. 2022;25(4): 39-47

Changes in white matter ultrastructure in aged mice corpora callosa

ARTICLE INFO

Article Type
Original Research

Authors

Elham Parandavar[1]

Mohammad Javan[2,3]*

1- Institute of Biochemistry and Biophysics, University of Tehran, Tehran, Iran
2- Department of Physiology, Faculty of Medical Sciences, Tarbiat Modares University, Tehran, Iran
3- Institute for Brain and Cognition, Tarbiat Modares University, Tehran, Iran.

***Corresponding author:**

Elham Parandavar

Mohammad Javan M.J.

Department of Physiology, Faculty of Medical Sciences, Tarbiat Modares University, Tehran, Iran.
Elham Parandavar: parandavar@ut.ac.ir
Mohammad Javan: mjavan@modares.ac.ir

Elham Parandavar and Mohammad Javan are jointly the corresponding authors.

ABSTRACT

Aging of can lead to significant cognitive and neurobehavioral deficits. In addition, aging leads to more susceptibility to neurological disorders, such as stroke, traumatic brain injury, and neurodegeneration. Accordingly, white matter (WM) changes associated with aging may be a factor in the functional impairment seen in the elderly. In this study, we initially determined whether the corpus callosum (CC) of old mice exhibited signs of cellular aging compared to young mice. To investigate cellular aging indices we examined SA-β-galactosidase and relative telomere length as markers of aging in the CC. Following this, we measured the myelination index through the g-ratio calculation. Our study demonstrated an increased g-ratio and axon diameter in aged mice. We also analyzed ultrastructural changes of myelinated axons and mitochondria in the CC of aged mice. The CC underwent substantial ultrastructural variation following the aging. These changes included myelination breakdown, the formation of myelin balloons, loss of the compact structure of myelin, and increased intramembrane density. we also investigated the impact of aging on mitochondria ultrastructure. We observed the presence of dark matrices and interconnected crista in a subgroup of the mitochondria in the CC. Such alterations are indicative of the deterioration in the integrity of WM with age. These findings are crucial as they provide insights into how aging affects the structural and functional aspects of WM, particularly in the CC. Understanding these changes is essential for developing strategies to mitigate age-related cognitive decline and to address the heightened susceptibility of aged WM to neurological disorders.

Key words: Aging; White matter; Myelin sheath; Cellular aging; Ultrastructure

INTRODUCTION

Brain aging is accompanied by cognitive decline in a significant portion of the population and is the primary risk factor for Alzheimer's disease (AD) and other common neurodegenerative disorders (Zia, Pourbagher-Shahri et al. 2021). As the brain ages, it undergoes various morphological alterations, including changes in gray and white matters (GM and WM, respectively), cerebral atrophy, volume loss, and ventricular enlargement (Dickstein, Kabaso et al. 2007). It is well-documented that the volume and weight of the brain decrease by approximately 5% per decade after the age of 40 (Peters 2006). This reduction in brain volume is associated with a decline in the number of neurons and the loss of synaptic connections, which are critical for cognitive functions. Normal brain aging is also linked with an unstable metabolic state, neuroinflammation, neuronal loss, and myelin degeneration (Mattson and Arumugam 2018). Neuroinflammation, characterized by the activation of glial cells and the release of pro-inflammatory cytokines, contributes to neuronal

damage and is a common feature in aging and neurodegenerative diseases. During aging, the cellular milieu of the brain exhibits epigenetic and translational changes, disturbances in proteostasis and autophagy, and cellular senescence (Sikora, Bielak-Zmijewska et al. 2021).

Cellular senescence, where cells cease to divide and function, increases in the aging brain, releasing inflammatory factors that exacerbate tissue damage and dysfunction. This process involves various molecular and cellular changes, such as DNA damage, telomere shortening, accumulation of damages, mitochondrial dysfunction, increased production of reactive oxygen species (ROS), and impaired lysosomal function (Chinta, Woods et al. 2015). These molecular and cellular alterations diminish the brain's ability to maintain homeostasis, so even the smallest disruptions can prevent the return to a balanced state, making the aging brain more susceptible to diseases and functional decline.

WM occupies a large volume of the cerebrum and is mainly composed of myelinated axons and myelin-producing glial cells (Dickstein, Kabaso et al. 2007). These myelinated axons within WM are crucial for efficient neurotransmission between the cortical and subcortical areas. As we age, myelinated nerve fibers in WM deteriorate both structurally and functionally, impairing communication between different parts of the central nervous system (CNS) (Blinkouskaya, Caçoilo et al. 2021). There are two distinct processes affecting white matter in aging: first, white matter atrophy and neuronal loss; second, the presence of white matter lesions (Vernooij, de Groot et al. 2008), which are signs of small vessel arteriolosclerosis, leading to incomplete ischemia, cell death (Liu, Yang et al. 2017). These lesions are associated with partial loss of myelin, axons, oligodendroglia cells, and mild reactive astrocytic gliosis (Schmidt, Schmidt et al. 2011).

The corpus callosum (CC) is the major white matter pathway interconnecting the left and right cerebral hemispheres located in the middle of the cerebrum (Frederiksen and Waldemar 2012). The CC consisted of 200-250 million contralateral axonal projections which play an essential role in the integration of lateralized sensory, cognition, and motor operation. The CC are susceptible to the aging process, and is associated with decline in cognition, attention allocation, sensory motor transfer (Reuter-Lorenz and Stanczak 2000) as well as progression of multiple sclerosis (MS) and AD (Granberg, Martola et al. 2015, Khasawneh, Abu-El-Rub et al. 2022). Moreover, because CC is a pure WM, crucial in connecting various brain regions, it has been extensively used to investigate age related WM changes and atrophy during aging and MS.

In this study, we aimed to prove the presence of cellular aging in old mice through structural changes in the CC by evaluating SA-β-galactosidase staining as well as the relative telomer length measurement as the prominent biomarkers of aging. Then we assessed myelination index through the g-ratio. Additionally, we examined ultrastructural changes in myelinated axons and mitochondria in the CC of aged mice.

Method

Animals

For our investigation, we used male C57BL6/J mice that were both young (2-month-old) and aged (18-month-old). We bought the young mice from the Pasteur Institute of Iran (Karaj, Iran). To supply older mice, 8-month-old mice were acquired from the same location and housed in the animal facility until they reached 18 months old. all mice were kept in standard cages with a 12-hour light/dark cycle at a temperature of 23 ± 2°C and provided with standard rodent chow and water ad libitum. The ARRIVE criteria were followed for all animal procedures and handling. Every effort was made to reduce the animals' suffering. All experimental protocols were approved by the Committee for Ethics in Animal Research of Tehran University Faculty of Sciences, Teran, Iran (Approval ID: IR.UT.SCIENCE.REC.1400.014).

Tissue preparation

For tissue sampling, mice were deeply anesthetized with an intraperitoneal injection of ketamine (Bremer Pharma GmbH) and xylazine (Kela), followed by transcardial perfusion with 0.1 M phosphate-buffered saline (PBS). Tissue preparation was done following the Cold Spring Harbor Laboratory protocol for cryosectioning

tissues (Rodig 2021). Brains were harvested, frozen in liquid nitrogen, embedded in optimal cutting temperature (OCT) compound (Bio-Optica), and cryosectioned at 10 µm thickness (Histo-Line Laboratories). All sections were stored at -70°C until use.

Senescence-associated β-galactosidase staining

To perform SA-β-gal staining, mice brain sections were fixed with 4% paraformaldehyde 2.5% glutaraldehyde for 10 minutes and then washed thrice with LacZ washing buffer (2 mM MgCl2, 0.01% Na Deoxycholate, and 0.02% Nonidet P-40) for 5 min. Consequently, the slides were stained overnight with freshly prepared LacZ staining solution at 37°C. LacZ staining solution contains 40 mM citric acid/Na phosphate buffer pH:5.6, 5 mM [K4Fe (CN)6. 3H2O], 5 mM K3[Fe (CN)6], 150 mM NaCl, 2 mM MgCl2, and 1 mg/ml X-gal (Bio Basic, Cat#BB0083) (n=3) (Debacq-Chainiaux, Erusalimsky et al. 2009). The images captured from the light microscopy. The percentage of SA-β-gal$^+$ cells was determined according to the artificial x-gal fluorescent signals made by ImageJ software to total cells stained by DAPI.

Electron microscopy

Mice were deeply anesthetized and perfused with pre-cooled 0.1 M sodium cacodylate buffer. The brain was sliced in matric and the CC were immediately separated and fixed in a pre-cooled 2.5% glutaraldehyde for 2 h at 4°C. Fixed tissue was washed twice in 0.1 M sodium cacodylate buffer, and to fix lipids were immersed in 1% osmium tetroxide for 90 min. then, the samples were dehydrated in serially increased ethanol concentration (25, 50, 70, 90 and 100%) 10 min each. Then tissue embedded in propylene oxide as resin solvent for 20 min and next in Agar resin (Agar Scientific Ltd)/propylene oxide as followed concentration (1:3, 1:1, 3:1 and 4:0) 2h each. To prepare the blocks tissues were embedded in pure resin at 60°C for 24h. The blocks were then sectioned into 50 nm ultrathin sections using an ultramicrotome type 4801A (LKB-producer AB-Stokholm) and placed on 300 mesh copper grid and double stained with 20% lead citrate and uranyl acetate for electron microscopic imaging using a transmission electron microscope (Hitachi HT-7800).

Toluidine blue staining

Toluidine blue (TB) used to visualize myelinated axons. Resin-embedded blocks were sectioned 1-2 µm thin by an ultramicrotome (C. Reichert, Austria). Sections were stained with 1% toluidine blue for 2 min at hot plate, and then washed with deionized water (Ghnenis, Czaikowski et al. 2018); slides evaluated under Olympus light microscopy BX-51. the g-ratio were calculated (the ratio of the axon diameter to the myelinated axon) using TB images. Each group included 3 mice and for each mouse, three sections were analyzed.

Relative telomer length measurement

One of the indicators of cellular aging and senescence is the reduction in telomere length, which can lead to errors during the replication of the DNA molecule's ends. For this assay, 4 mice brain tissues were homogenized separately, and DNA was isolated using the standard phenol/chloroform extraction method. DNA quantitation was performed using a nanodrop spectrophotometer (Thermo Scientific). Samples having 260/280 absorbance ratios ≥1.8 were considered pure DNA. RT-qPCR was employed for both telomer and control 36b4r quantification using RealQ plus 2x master mix green (Ampliqon, Cat# A325402), on a Rotor-Gene device (Qiagen). The primer sequences for telomer F were (5′-CGGTTTGTTTGGGTTTGGGTTTGGGTTTG GG TTTGGGTT -3′) and telomer R were 36b4f F (5′- ACTGGTCTAGGACCCGAGAAG -3′) and 36b4f R (5′- TCAATGGTGCCTCTGGAGATT ′) (O'Callaghan and Fenech 2011). The PCR profile included an initial heating for 10 minutes at 95°C, followed by 40 amplification cycles, each consisting of 15 seconds at 95°C and 60 seconds at 60°C. The telomere to 36b4 ratio was calculated using the 2-ΔCT method (n=4-6).

Result

Senescence associated aging in CC

Age, as an irreversible process, restricts tissue regeneration and impairs CNS remyelination (Yankner, Lu and Loerch 2008).We hypothesized that the cellular aging may contribute to differences in support for myelination. First, we

determined the activity of lysosomal enzyme β-gal, as a marker of cellular senescence by SA-β-gal staining (Fig. 1A). The SA–β-gal positive cells were elevated 8.3% (*p< 0.001*) in Aged mice (18-month-old) CCS compared to Young (2-month-old) mice (Fig. 1B). We also measure telomer length relatively which also decrease by cellular senescence. our results revealed a relative 1.46 decrease in telomer length (p< 0.001) in Aged mice. This emphasis presence of cellular aging in 18 months old mice.

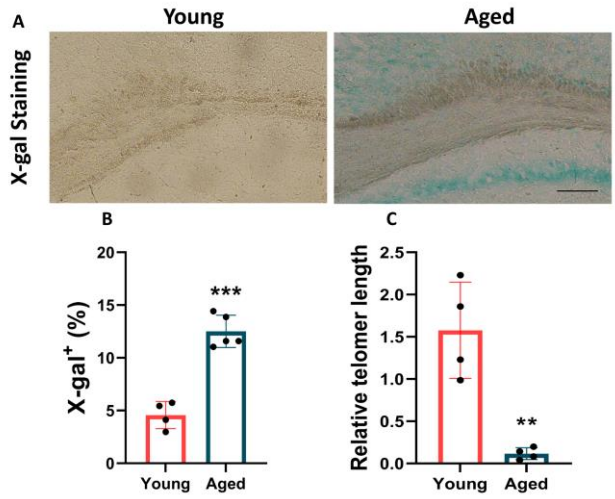

Figure 1: Aging Causes Cell Senescence. (A) SA-β-gal staining, a marker of cell cycle arrest, in the corpus callosum (CC) of young and aged mice revealed an increase in SA-β-gal with aging. **(B)** Quantification of the percentage of SA-β-gal+ cells in the CC of young and aged mice. **(C)** Quantification of relative telomere length in young and aged mice, showing a decrease in telomere length with aging. Statistical analyses were t.test. All experiments were conducted in triplicate, with n=4-5 mice per group. * Represents the comparison between young and aged groups. ** p=0.002, *** p < 0.0001 between conditions.

Alteration in myelination index during aging

To analyze WM alteration throughout life, semi-thin sections of the CCs region were stained with TB. Micrographs from Young and Aged groups are presented in Figure 2.A. The micrographs were analyzed to measure the g-ratio, axon diameter, and the number of axons. The g-ratio, an appropriate index for studying the extent of myelination, is defined as the ratio of inner to outer diameter of myelinated axon, is associated with the speed of conduction, and thus reflects axonal function and integrity. In Figure 2.B g-ratio index was compared between young and aged mice (Young: slope 0.3378, y-intercept 0.5565, $n = 259$ axons, $n = 3$ mice, Aged: slope 0.3282, y-intercept 0.4559, $n = 309$, $n = 3$ mice, slopes $p = 0.75$, intercept $p < 0.001$.).

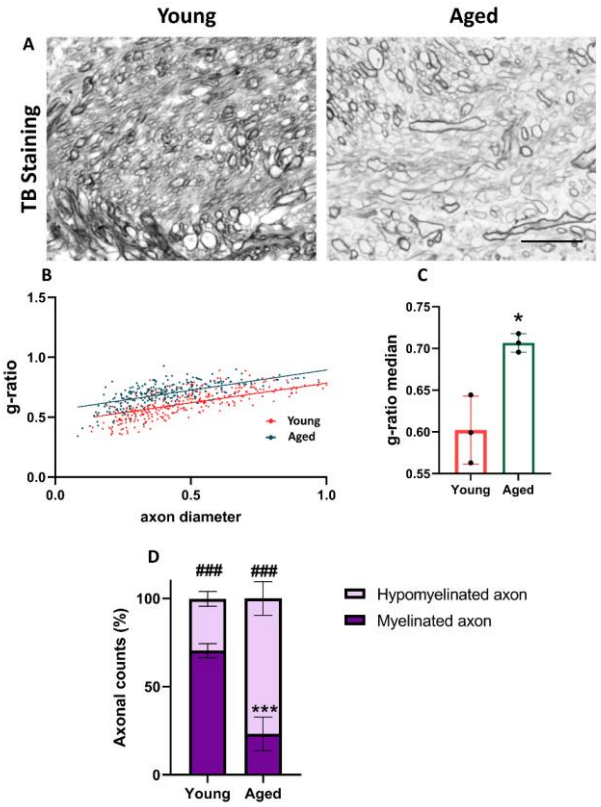

Figure 2: Myelin Ensheathment Altered by Aging. (A) representative images of toluidine blue staining of semithin sections of the corpus callosum (CC) in Young and Aged mice, scale bar 10 µm. **(B)** Scatter plot showing the g-ratio per axon diameter, indicating an increase in the g-ratio with aging. Using ImageJ software, the g-ratio was computed by dividing the inner axonal diameter by the myelinated axon diameter determined in each grided segment. Three separate sections of the CC were examined for each mouse. **(C)** Column plot showing median changes in the g-ratio, indicating an increase in the g-ratio over the lifespan. **(D)** Quantification of the percentage of axons in 100 µm² of toluidine blue-stained images, distinguishing between the percentage of myelinated axons (g-ratio ≤ 0.6) and hypomyelinated axons (g-ratio > 0.6) in Young and Aged mice. Statistical analyses were performed using a t-test for (C) and two-way ANOVA with Šídák's multiple comparisons tests for (D). All experiments were conducted in triplicate, with n=3 mice per group. * Represents comparison between young and aged mice, # represents comparison between myelinated and hypomyelinated axons. * p=0.01, *** or ### p < 0.001 between conditions.

Evaluating changes in g-ratio median shows a significant increase in in Aged mice (0.1, p= 0.012) compared to Young groups (Figure 2.C). As the g-ratio average and its standard deviation were 0.64 in Young group, we considered axons with a g-ratio of less than or equal to 0.64 to be myelinated and the remaining axons to be hypomyelinated. In both young and aged mice, we examined the percent of myelinated and hypomyelinated axons (Figure 2.D). The young mice had a considerably larger percentage of myelinated axons (46.78%, p<0.001), compared to the aged group. These results suggest that myelin content reduces with age.

Myelin ultrastructure Changes in aging

We performed an ultrastructural study on CC sections from the aged group using transmission electron microscopy (TEM). As shown in Figures 3A and 3B, the evaluation of CCs in aged mice revealed significant ultrastructural alterations in myelin structure. We observed localized degeneration of myelin sheaths in some axons (indicated by D in Figure 3.A, B), which could be attributed to a decrease in myelination with increasing age. The compact and dense structure of myelin surrounding the axons was notably affected. There was evidence of splitting of the myelin lamellae (indicated by S in Figure 3.A, B) in certain regions around the axon. This splitting could lead to the bulging out of cytoplasm, a structural alteration of myelin associated with aging known as myelin balloons (indicated by B in Figure 3.A, B). These findings suggest that aging significantly impacts the integrity of the myelin sheath, resulting in structural deformities that could impair nerve function. The observed degenerative changes, including myelin splitting and balloon formation, highlight the vulnerability of the myelin sheath to age-related deterioration, which may contribute to the overall decline in neural function seen in aged organisms.

Mitochondrial morphological Changes in aging

Mitochondrial dysfunction is a major driving force in aging (Trifunovic and Larsson 2008, Elfawy and Das 2019). We evaluated mitochondrial features in the brain sections following aging. The ultrastructural examination of CC exhibited a significant alteration in the mitochondrial ultrastructure in aged mice, which is indicated by M (Figure 4.A, B). Based on the evidence, some mitochondria had a normal appearance with parallel crista and normal matrix density, while others showed variations in the internal organization, such as some with disrupted cristae structures that filled the entire internal space of the mitochondria with branched and interconnected crista. In these mitochondria, we also saw significant matrix density and irregular junction.

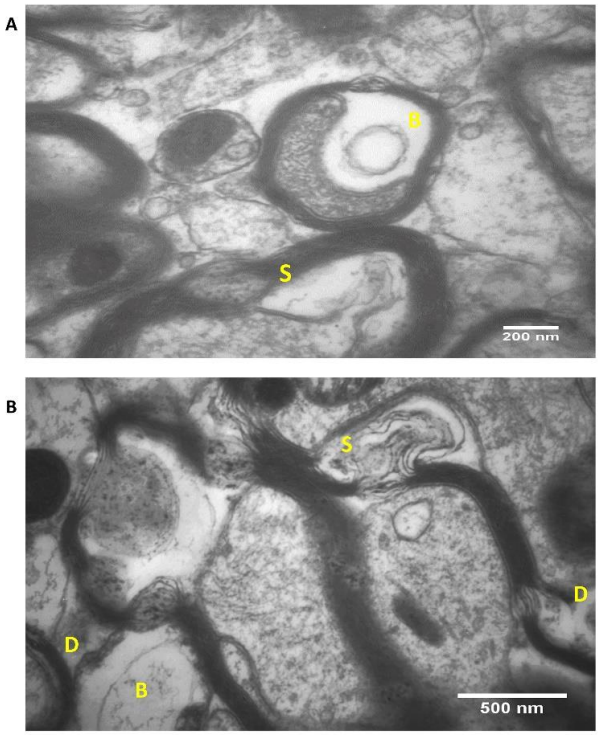

Figure 3: Ultrastructural features of aging in the Corpus Callosum (CC). (A, B) Transmission electron microscopy (TEM) images of the CC in aged mice, showing myelin splitting (indicated by S), myelin balloon formation (indicated by B), and myelin degeneration (indicated by D).

We also compared the surface area of mitochondria in the young and aged mice (Figure 4. C). We categorized the mitochondria smaller than 0.03 square micrometers as small, medium (0.03-0.075 μm^2), large (0.076-0.155 μm^2), and those larger than 0.156 square micrometers as very large. As shown in Figure 4.C, only the frequency of very large mitochondria revealed a significant difference (p< 0.001) between the

Young and Aged groups. The percentage of the mitochondria with various surface areas was also displayed (Figure 4.D). It appears that mitochondria with a surface area of 0.02-0.06 are the most frequent in the Young and, the mitochondria with a surface area of 0.04-0.08 are more prevalent in the Aged mice.

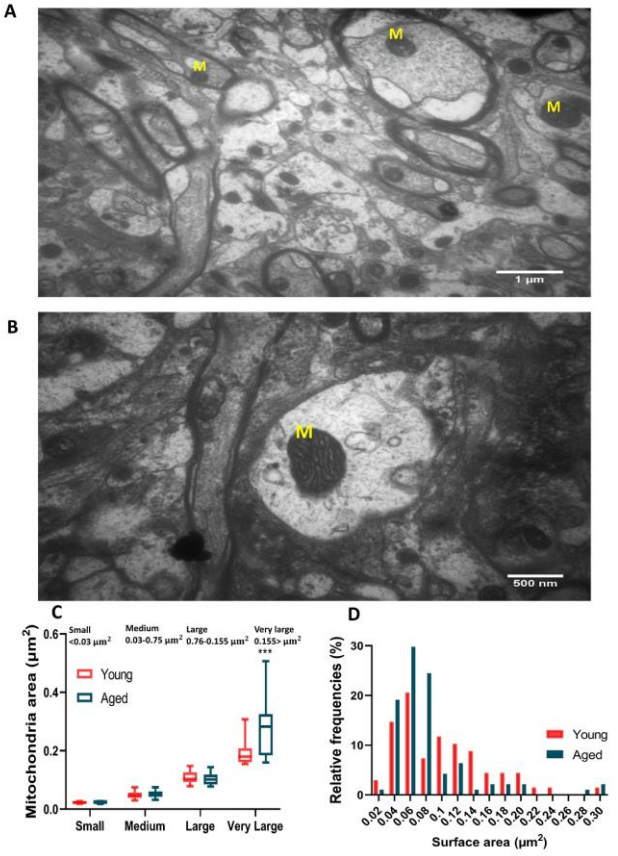

Figure 4: Mitochondrial alteration during aging in the Corpus Callosum (CC). (A, B) Representative transmission electron microscopy (TEM) images of the CC from aged mice, showing mitochondria (indicated by M) in the aged group. (C, D) Age-dependent cha

Discussion

Previous studies have well established that cellular senescence acts as a significant factor in the progression of the aging in mammals (Kumari and Jat 2021). This may be due to the activity of senescent cells as a continuous source of cell cycle arrest signals and pro-inflammatory factors, leading to the loss of homeostasis and function in various body parts (Jurk, Wang et al. 2012). Our study results show an increase in SA-β-gal+ cells in the CC of aged mice, which is most widely used for detecting the senescent cells. A relative reduction in telomere length was also observed in aged group, suggesting cell cycle arrest and cellular senescence occurrence in the18-month-old mice. Reports indicate that telomere shortening as a biological biomarker of aging is related to neurodegenerative disease like AD and PD as well as MS (Krysko, Henry et al. 2019, Rodríguez-Fernández, Gispert et al. 2022).

This study examined changes in the myelin sheath throughout aging of mice. Through adulthood, the function of the myelin sheaths, which envelop axons and provide effective saltatory conductivity and metabolic support, steadily declines, affecting total brain activity (Salzer and Zalc 2016). Our data showed a decrease in myelin content in aged mice (Figure 2). Another study in the cortex of 18-month-old mice reported the same decline in myelin content (Wang, Ren et al. 2020). our results demonstrate a significant increase in axon diameter and a decrease in myelin thickness, which is reflected as an increase in the g-ratio. These findings are consistent with previous reports showing changes in the g-ratio in WM related to aging (Xie, Liang et al. 2014). Furthermore, in our work, we established a g-ratio index of 0.64 to examine the myelinated and hypomyelinated axons. A previous study (West, Kelm et al. 2015) found that the g-ratio of the mouse CC from electron microscope images was 0.6±0.04 in young mice. Aging causes a reduction in the proportion of myelinated axons in the CC. Loss of white matter has been observed in many neurodegenerative diseases in the elderly as well as normal aging (Marner, Nyengaard et al. 2003, Nasrabady, Rizvi et al. 2018).

Electron microscopy studies have established the changes in myelinated nerve fiber morphology as a major alteration observed during normal aging (Stadelmann, Timmler et al. 2019). It is suggested that such degenerative changes lead to cognitive decline because they cause changes in conduction velocity, resulting in a disruption of the normal timing in neuronal circuits(Xie, Liang et al. 2014). we observed an increased prevalence of abnormal myelin appearance in the CC, such as myelin

degeneration, loss of compact structure of myelin, splitting of myelin lamellae, presence of myelin balloons, and lower myelin content in aged mice.

Mitochondrial disfunction is a key player in induction of aging. Studies on the mitochondria of mice and yeast reveal that abnormal cristae shape caused by defect in the ATP synthase's molecular organization (Davies, Anselmi et al. 2012, Mourier, Ruzzenente et al. 2014). However, the impact of aging on mitochondrial morphology is not fully understood, previous studies of the ultrastructure of mitochondria in mouse heart by TEM revealed anomalous and inter connected cristae in the mitochondria and elongation in mitochondrial length by aging (Brandt, Mourier et al. 2017). Our experiment detected irregular structure of mitochondria in aged mice. The morphological changes in the mitochondria, such as packed lamellar cristae resulting in a spiral-like cristae network, and the dense matrices are important aging features of aged Drosophila and CA1 part of aged rat brains (Jiang, Lin et al. 2017, Rybka, Suzuki et al. 2019). Additionally, we evaluated the surface area of mitochondria in both young and old mice in TEM micrographs. It seemed that as mice had aged, the frequency of larger mitochondria was increased.

The importance of how WM ages under normal conditions and in clinical manifestations of neurodegenerative diseases has been greatly underestimated. Study alteration the morphology of myelinated nerve fibers using electron microscope images is introduced as a fundamental indicator of aging in the central nervous system. Here, structurally changed myelinated axons indicate extensive damage to the axons and myelin sheaths. Our results also suggest that aging interrupt mitochondrial function which could lead to ATP depletion and increased oxidative stress in WM. Consequently, interventions that attenuate oxidative injury, preserve mitochondrial structure and function, and restore ATP levels effectively promote axon function recovery, even when applied after ischemia (Baltan 2013).

Further investigations are required to determine the impact of the age-dependent changes in WM structure and myelin degeneration in disease models such as glaucoma, multiple sclerosis, traumatic brain injury, and AD.

All experimental protocols were approved by the Committee for Ethics in Animal Research of Tehran University Faculty of Sciences, Teran, Iran (Approval ID: IR.UT.SCIENCE.REC.1400.014).

Abbreviations

AD: Alzheimer Disease, CC: Corpus Callosum, CNS: Central Nervous System, MS: Multiple Sclerosis, TB: Toluidine Blue, WM: White Matter.

References:

[1] Baltan, S. (2013). Age-dependent mechanisms of white matter injury after stroke. White matter injury in stroke and CNS disease, Springer**:** 373-403.

[2] Blinkouskaya, Y., A. Caçoilo, T. Gollamudi, S. Jalalian and J. Weickenmeier (2021). "Brain aging mechanisms with mechanical manifestations." Mechanisms of ageing and development **200**: 111575.

[3] Brandt, T., A. Mourier, L. S. Tain, L. Partridge, N.-G. Larsson and W. Kühlbrandt (2017). "Changes of mitochondrial ultrastructure and function during ageing in mice and Drosophila." Elife **6**: e24662.

[4] Davies, K. M., C. Anselmi, I. Wittig, J. D. Faraldo-Gómez and W. Kühlbrandt (2012). "Structure of the yeast F1Fo-ATP synthase dimer and its role in shaping the mitochondrial cristae." Proceedings of the National Academy of Sciences **109**(34): 13602-13607.

[5] Debacq-Chainiaux, F., J. D. Erusalimsky, J. Campisi and O. Toussaint (2009). "Protocols to detect senescence-associated beta-galactosidase (SA-βgal) activity, a biomarker of senescent cells in culture and in vivo." Nature protocols **4**(12): 1798-1806.

[6] Dickstein, D. L., D. Kabaso, A. B. Rocher, J. I. Luebke, S. L. Wearne and P. R. Hof (2007). "Changes in the structural complexity of the aged brain." Aging cell **6**(3): 275-284.

[7] Elfawy, H. A. and B. Das (2019). "Crosstalk between mitochondrial dysfunction, oxidative stress, and age related neurodegenerative disease: Etiologies and therapeutic strategies." Life sciences **218**: 165-184.

[8] Frederiksen, K. S. and G. Waldemar (2012). "Corpus callosum in aging and neurodegenerative

diseases." Neurodegenerative Disease Management **2**(5): 493-502.

[9] Ghnenis, A. B., R. E. Czaikowski, Z. J. Zhang and J. S. Bushman (2018). "Toluidine blue staining of resin-embedded sections for evaluation of peripheral nerve morphology." JoVE (Journal of Visualized Experiments)(137): e58031.

[10] Granberg, T., J. Martola, G. Bergendal, S. Shams, S. Damangir, P. Aspelin, S. Fredrikson and M. Kristoffersen-Wiberg (2015). "Corpus callosum atrophy is strongly associated with cognitive impairment in multiple sclerosis: results of a 17-year longitudinal study." Multiple Sclerosis Journal **21**(9): 1151-1158.

[11] Jiang, Y.-f., S.-s. Lin, J.-m. Chen, H.-z. Tsai, T.-s. Hsieh and C.-y. Fu (2017). "Electron tomographic analysis reveals ultrastructural features of mitochondrial cristae architecture which reflect energetic state and aging." Scientific Reports **7**(1): 45474.

[12] Jurk, D., C. Wang, S. Miwa, M. Maddick, V. Korolchuk, A. Tsolou, E. S. Gonos, C. Thrasivoulou, M. Jill Saffrey and K. Cameron (2012). "Postmitotic neurons develop a p21-dependent senescence-like phenotype driven by a DNA damage response." Aging cell **11**(6): 996-1004.

[13] Khasawneh, R. R., E. Abu-El-Rub, A. Alzu'bi, G. T. Abdelhady and H. S. Al-Soudi (2022). "Corpus callosum anatomical changes in Alzheimer patients and the effect of acetylcholinesterase inhibitors on corpus callosum morphometry." Plos one **17**(7): e0269082.

[14] Krysko, K. M., R. G. Henry, B. A. Cree, J. Lin, S. F. M. E. T. University of California, S. Caillier, A. Santaniello, C. Zhao, R. Gomez and C. Bevan (2019). "Telomere length is associated with disability progression in multiple sclerosis." Annals of neurology **86**(5): 671-682.

[15] Kumari, R. and P. Jat (2021). "Mechanisms of Cellular Senescence: Cell Cycle Arrest and Senescence Associated Secretory Phenotype." Front Cell Dev Biol **9**: 645593.

[16] Liu, H., Y. Yang, Y. Xia, W. Zhu, R. K. Leak, Z. Wei, J. Wang and X. Hu (2017). "Aging of cerebral white matter." Ageing Res Rev **34**: 64-76.

[17] Marner, L., J. R. Nyengaard, Y. Tang and B. Pakkenberg (2003). "Marked loss of myelinated nerve fibers in the human brain with age." Journal of comparative neurology **462**(2): 144-152.

[18] Mattson, M. P. and T. V. Arumugam (2018). "Hallmarks of Brain Aging: Adaptive and Pathological Modification by Metabolic States." Cell Metab **27**(6): 1176-1199.

[19] Mourier, A., B. Ruzzenente, T. Brandt, W. Kühlbrandt and N.-G. Larsson (2014). "Loss of LRPPRC causes ATP synthase deficiency." Human molecular genetics **23**(10): 2580-2592.

[20] Nasrabady, S. E., B. Rizvi, J. E. Goldman and A. M. Brickman (2018). "White matter changes in Alzheimer's disease: a focus on myelin and oligodendrocytes." Acta Neuropathol Commun **6**(1): 22.

[21] O'Callaghan, N. J. and M. Fenech (2011). "A quantitative PCR method for measuring absolute telomere length." Biological procedures online **13**: 1-10.

[22] Peters, R. (2006). "Ageing and the brain: This article is part of a series on ageing edited by Professor Chris Bulpitt." Postgraduate medical journal **82**(964): 84-88.

[23] Reuter-Lorenz, P. A. and L. Stanczak (2000). "Differential effects of aging on the functions of the corpus callosum." Developmental neuropsychology **18**(1): 113-137.

[24] Rodig, S. J. (2021). "Preparing frozen tissue sections for staining." Cold Spring Harbor Protocols **2021**(3): pdb. prot099655.

[25] Rodríguez-Fernández, B., J. D. Gispert, R. Guigo, A. Navarro, N. Vilor-Tejedor and M. Crous-Bou (2022). "Genetically predicted telomere length and its relationship with neurodegenerative diseases and life expectancy." Computational and Structural Biotechnology Journal **20**: 4251-4256.

[26] Rybka, V., Y. J. Suzuki, A. S. Gavrish, V. A. Dibrova, S. G. Gychka and N. V. Shults (2019). "Transmission electron microscopy study of mitochondria in aging brain synapses." Antioxidants **8**(6): 171.

[27] Salzer, J. L. and B. Zalc (2016). "Myelination." Curr Biol **26**(20): R971-R975.

[28] Schmidt, R., H. Schmidt, J. Haybaeck, M. Loitfelder, S. Weis, M. Cavalieri, S. Seiler, C. Enzinger, S. Ropele and T. Erkinjuntti (2011). "Heterogeneity in age-related white matter changes." Acta neuropathologica **122**: 171-185.

[29] Sikora, E., A. Bielak-Zmijewska, M. Dudkowska, A. Krzystyniak, G. Mosieniak, M. Wesierska and J. Wlodarczyk (2021). "Cellular senescence in

brain aging." Frontiers in aging neuroscience **13**: 646924.

[30] Stadelmann, C., S. Timmler, A. Barrantes-Freer and M. Simons (2019). "Myelin in the central nervous system: structure, function, and pathology." Physiological reviews **99**(3): 1381-1431.

[31] Trifunovic, A. and N. G. Larsson (2008). "Mitochondrial dysfunction as a cause of ageing." Journal of internal medicine **263**(2): 167-178.

[32] Vernooij, M. W., M. de Groot, A. van der Lugt, M. A. Ikram, G. P. Krestin, A. Hofman, W. J. Niessen and M. M. Breteler (2008). "White matter atrophy and lesion formation explain the loss of structural integrity of white matter in aging." Neuroimage **43**(3): 470-477.

[33] Wang, F., S.-Y. Ren, J.-F. Chen, K. Liu, R.-X. Li, Z.-F. Li, B. Hu, J.-Q. Niu, L. Xiao and J. R. Chan (2020). "Myelin degeneration and diminished myelin renewal contribute to age-related deficits in memory." Nature neuroscience **23**(4): 481-486.

[34] West, K. L., N. D. Kelm, R. P. Carson and M. D. Does (2015). "Quantitative analysis of mouse corpus callosum from electron microscopy images." Data in brief **5**: 124-128.

[35] Xie, F., P. Liang, H. Fu, J. C. Zhang and J. Chen (2014). "Effects of normal aging on myelin sheath ultrastructures in the somatic sensorimotor system of rats." Molecular Medicine Reports **10**(1): 459-466.

[36] Yankner, B. A., T. Lu and P. Loerch (2008). "The aging brain." Annu Rev Pathol **3**: 41-66.

[37] Zia, A., A. M. Pourbagher-Shahri, T. Farkhondeh and S. Samarghandian (2021). "Molecular and cellular pathways contributing to brain aging." Behavioral and Brain Functions **17**(1): 6.